

## Article

# The Characteristics of Lipid Biomarkers from the Abyssal and Hadal Sediments of the Yap Trench and the Influence of V-Shape Topography

Aftab Hussain Khuhawar<sup>1,2</sup>, Chengjun Sun<sup>3</sup> , Gui-Peng Yang<sup>1,2,4</sup> and Haibing Ding<sup>1,2,4,\*</sup> 

- <sup>1</sup> Frontiers Science Center for Deep Ocean Multispheres and Earth System, Key Laboratory of Marine Chemistry Theory and Technology, Ministry of Education, College of Chemistry and Chemical Engineering, Ocean University of China, Qingdao 266100, China
- <sup>2</sup> Qingdao National Laboratory for Marine Science and Technology, Qingdao 266237, China
- <sup>3</sup> Marine Ecology Center, First Institute of Oceanography of State Oceanic Administration, Qingdao 266061, China
- <sup>4</sup> Qingdao Collaborative Innovation Center of Marine Science and Technology, Qingdao 266100, China
- \* Correspondence: dinghb@ouc.edu.cn

**Abstract:** Lipid biomarkers from deep-sea sediments have been observed in several studies, but little is known about their occurrence in trench system sediments. Here, we determined the concentrations of lipid biomarkers (fatty acids and neutral lipids) in sediments from the north Yap Trench. Our results showed that short-chain (C12–20) saturated fatty acids (SFAs) contributed more than (C12:1–23:1) monounsaturated fatty acids (MUFAs), and (C16:3–24:4) polyunsaturated fatty acids (PUFAs). Most fatty acids (FAs) suggest that bacteria and algae were the main contributors to marine organic matter. In contrast, terrestrial organic matter (OM) was a minor contributor to long carbon chain fatty acids greater than C20. On the other side, the observed neutral lipids such as alkanes (C14–C27), alkanols (C12–C20), alkenes (C17:1–C26:1), phytol and sterol (C27–29) indicate that phytoplankton and bacteria were the main contributors of organic materials in the sediments, and the carbon chain of neutral lipids C20–29 offering the sources of terrestrial organic matter. The extremely depleted  $\delta^{13}\text{C}$  values of fatty acids give the sources of organic carbon in the sediments from bacteria, algae, and methane-related microbes. This study is important for understanding the biogeochemical activities in deep-sea environments, particularly in the abyss and hadal zones. It will be helpful to understand the sources, transfer, and deposition of organic matter in marine trenches.

**Keywords:** abyss; hadal zone; fatty acids; neutral lipids;  $\delta^{13}\text{C}$  value



**Citation:** Khuhawar, A.H.; Sun, C.; Yang, G.-P.; Ding, H. The Characteristics of Lipid Biomarkers from the Abyssal and Hadal Sediments of the Yap Trench and the Influence of V-Shape Topography. *Water* **2022**, *14*, 3111. <https://doi.org/10.3390/w14193111>

Academic Editor: Luisa Bergamin

Received: 9 August 2022

Accepted: 28 September 2022

Published: 2 October 2022

**Publisher's Note:** MDPI stays neutral with regard to jurisdictional claims in published maps and institutional affiliations.



**Copyright:** © 2022 by the authors. Licensee MDPI, Basel, Switzerland. This article is an open access article distributed under the terms and conditions of the Creative Commons Attribution (CC BY) license (<https://creativecommons.org/licenses/by/4.0/>).

## 1. Introduction

The abyssal 4000–6000 m and hadal 6000–11,000 m zones are the deepest and least explored aquatic biospheres in the world. In contrast to abyssal settings, the hadal environments have high hydrostatic pressure and distinct topography and geomorphology [1]. Advances in deep-sea technologies have sparked interest in studying the trenches and urged a re-evaluation of abyssal and hadal ecology in recent decades. The Yap Trench is one of the deepest trenches (8552 m) with typical abyssal and hadal environments located in the southeastern section of the Philippine Sea in the Western Pacific Ocean. The “V” shape topography and hydrothermal activity in the Yap Trench significantly impact the concentrations and distributions of numerous chemicals in sediments, especially for organic matter [2], which is an ideal place to study the organic carbon cycle in an extreme marine environment [3].

As an illustration, owing to the remote location from major landmasses, the organic components present in the sediment of the Yap Trench, the Japan Trench, and the Mariana Trench are primarily sourced from marine phytoplankton, and terrestrial organism sources

barely exist [4,5]. A considerable quantity of allochthonous terrigenous organic material was found in the New Britain Trench and the Izu-Bonin Trench, which are relatively close to big islands [6,7]. Large amounts of sedimentary matter are transported from the nearby margin to the abyssal and the hadal trench by mass-wasting events brought by tectonically formation [8,9]. Compared to the nearby abyssal plains, the sediments in the hadal zone showed higher rates of organic carbon buildup, increased microbial activity, and higher benthic biomass [6,10,11]. A trench funnel or V-shape topography makes it simple to capture settling particle matter brought in by turbidity currents, natural sedimentation, and ocean circulation [12,13]. As a result, the hadal zone is considered a depocenters for sediments and organic material in conjunction with the increased diagenetic activity presented in such a harsh environment compared to the abyss [6,14,15]. A general trench topography is shown in Figure 1.

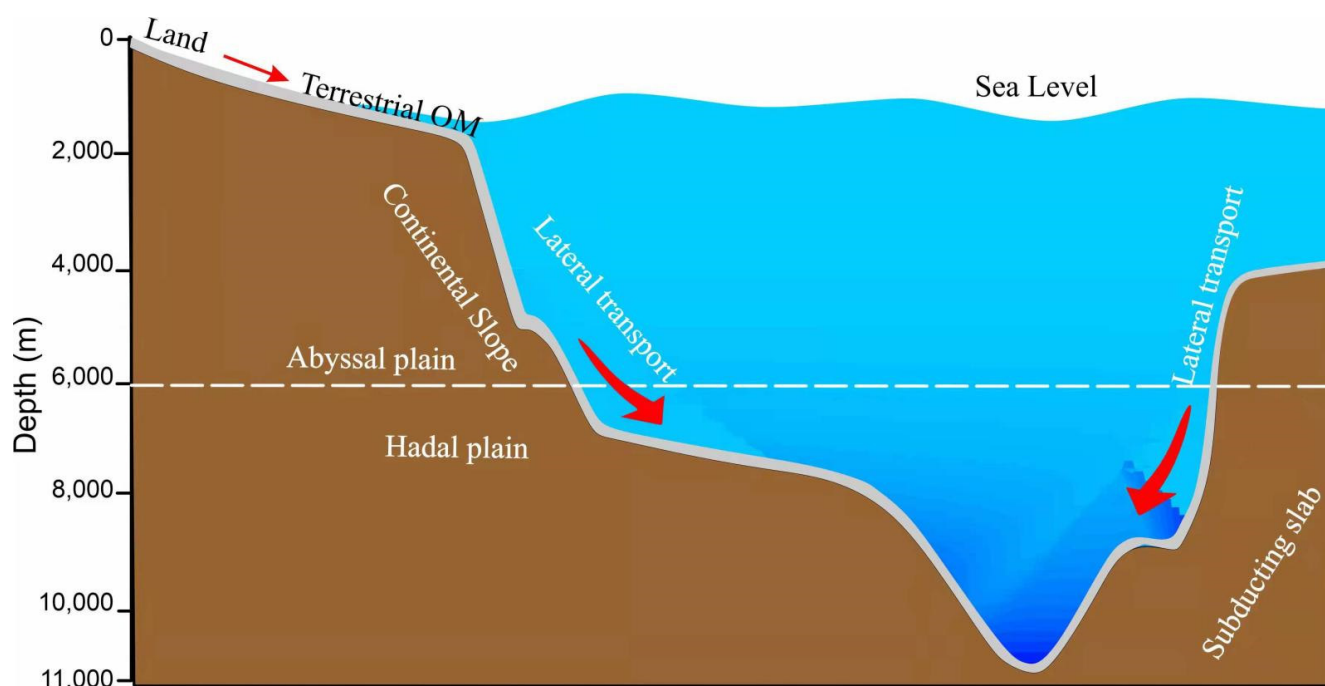


**Figure 1.** The level of depth, transport, and sources of organic matter in the Yap trench.

There has been a lot of focus on finding sources of organic matter in the trench environment [1]. The organic-rich particulate matter is significant in providing food and nutrients in the trench environment [16,17] and adding dead marine life and upper ocean corpses [8]. Organic material in trench sediments comes from either marine or terrestrial sources. Their respective proportions are influenced mainly by the surface productivity of oceans, the water depth, and geographical positions. Between abyssal and hadal environments, Jamieson et al. [18] found a significant variation in diversity, fertility, and biomass of benthic epifaunal and infaunal invertebrates. The biomass drops with depth due to a lack of food and strong hydrostatic pressure at bathyal and abyssal depths [19,20].

The organic matter preserved in marine sediments keeps extensive evidence concerning historic environment records, such as past productivity, paleoclimate change, paleo-environmental conditions, genetic information, and knowledge about microbes and food sources [21–23]. Lipid biomarkers and  $^{13}\text{C}$  stable isotope are two widely used methods to track organic matter in marine sediments. It is well acknowledged that organic substances made from various critical sources by numerous synthetic processes in different environments may all have several isotopic compositions. As a result, it is common to use the isotopic compositions of particular compounds to determine the biological origin of the compounds and the depositional environment [24,25]. In this study, numerous lipid biomarkers such as fatty acids (FAs), their  $\delta^{13}\text{C}$  values, and neutral lipids were determined

to provide an inclusive insight into the intrinsic arrangement of organic matter (OM). The lipids were attentive to reveal the characteristics of organic matter from sediments of abyssal and hadal areas of the Yap Trench and were applied to investigate the relationship between the lipid biomarkers and the change of ecosystem in a deep-sea environment, especially in the abyss and the hadal zone.

## 2. Materials and Methods

### 2.1. Study Area of the Yap Trench

The Yap Trench is located at the east side of the Yap Ridge and the Yap Islands. The trench is about 700 km long and 50 km wide, forming a “J” shape towards the southeast [26]. Between the northern end of the Yap Trench and the southern end of the Mariana Trench, a typical trench–trench junction forms at a roughly perpendicular angle near 11°07' N, which is the convergence of the Philippine Sea Plate, the Pacific Plate, and the Caroline Plates [27]. Its north section is significantly affected by the three plates. As a comparison, its south section is mainly affected by the Caroline Plates and the Philippine Sea Plate, which is obviously different from the north section. The two sections are separated at 8°26' N [28]. There is no active volcanism in the Yap Island Arc [29,30]. Whereas McCabe and Uyeda (1983) [31] proposed that the collision of the Caroline Ridge with the trench has suspended subduction at its northern section in light of tectonic features. According to earlier research by Song et al. (2016) [32], the trench experienced frequent micro-earthquakes, a high heat flow value, and possible small-scale hydrothermal activity on its western side [3]. Two slope breaks on the higher landward slope and normal faults, horsts, and grabens on the descending oceanward slope were also plainly visible in previous geophysical data [33]. Weak seismic activity is a characteristic of the trench as defined by Wenzhöfer et al. (2016) [34]. The water column of the Yap Trench is characterized by relatively cold (1–2 °C) Antarctic Circumpolar Deep Water. The northern Yap Trench has periodic internal tides and inertial currents [35].

### 2.2. Sampling Stations

In May 2016, the “Jiaolong” manned submersible implemented an experimental voyage. The multi-tube sampler obtained two sediment core samples (Table 1 and Figure 2) from the north Yap Trench. Both sediment samples were 10 cm long. The abyssal core sample (from station S01) was taken from the depth of 5058 m, having black iron-manganese nodules. The hadal core sample (from station D113) was taken from the depth of 6578 m and was dark brown and muddy. The top 8 cm sediment of each sample was sliced into eight subsamples with an interval of 1 cm, placed in a combusted aluminum foil bag, and preserved at −20 °C until further analysis.

**Table 1.** Sampling stations and their depth.

Sampling Stations	Sampling Location	Depth of Station (m)	Longitude	Latitude
S01	East side of the trench cliff	5058	138°40.86'	9°39.67'
D113	East side of the trench cliff	6578	138°39.41'	9°51.93'

### 2.3. Extraction of Lipid Compounds

For the extraction of neutral lipids and fatty acids, a modified method from Yan, et al. (2020) [2] was followed. The concentrations of lipids in the sediment were calculated based on dry sediment weight. The water content of the sediment subsamples was determined by the oven drying method. For each subsample, about 0.5 g of sediment were weighed and heated in an oven at 100 °C for 24 h. The water content was obtained according to the difference of the sediment weight before and after drying.

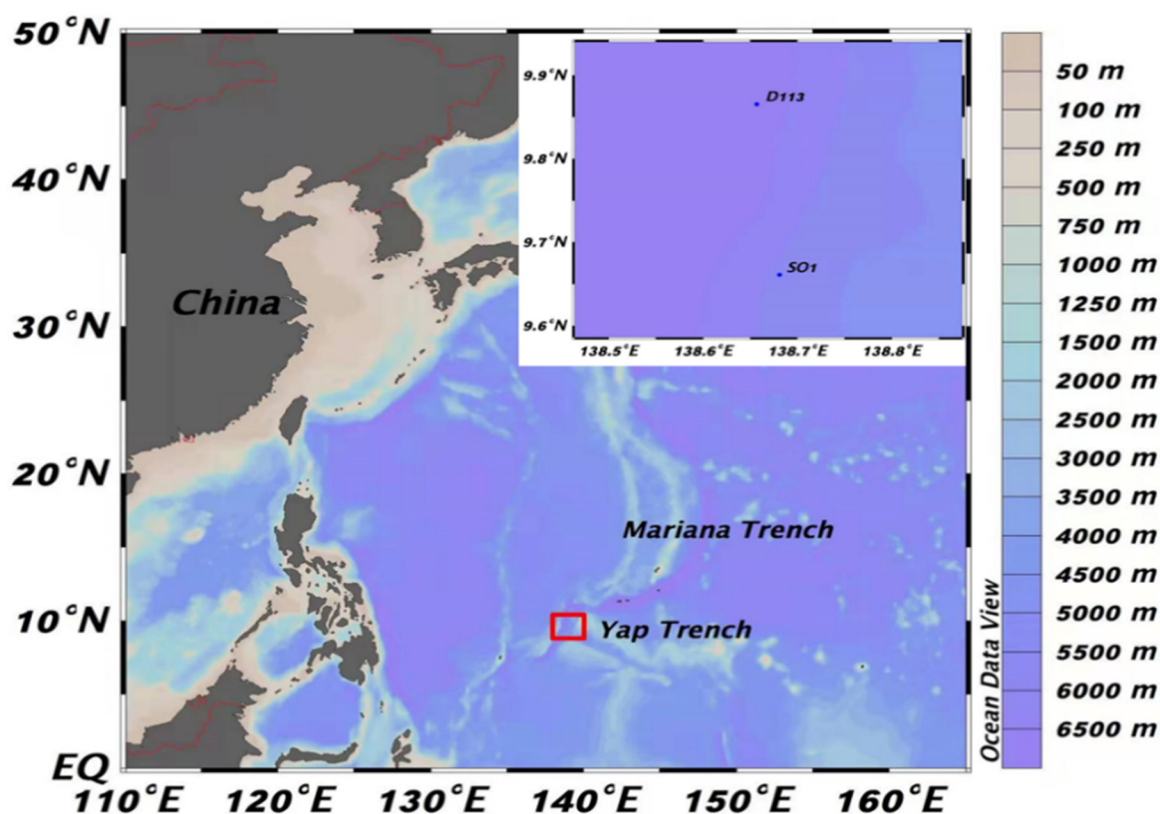


Figure 2. The location map and the sampling stations of the Yap Trench.

For neutral lipids and fatty acids extraction, each sediment subsample was weighed 1–2 g in a centrifuge tube. Then, approximately 10 mL of MeOH was added to the centrifuge tube, carried out to 1 min vortex, and sonicated for 4 min. Next, the sample was put into a centrifuge machine at 2500 rounds per min (rpm) for 8 min. After centrifugation, the supernatant was transferred to a separatory funnel. Then,  $3 \times 10$  mL of  $\text{CH}_2\text{Cl}_2$ -MeOH solution ( $v/v = 2:1$ ) was used for three more extractions. All the supernatant was transferred to the separatory funnel. A small quantity of 5% sodium chloride (NaCl) solution was added to promote the formation of organic and inorganic phases. Subsequently, standing for 6 h, the lower organic layer was separated into a 100-mL pyriform flask. The supernatant in the separatory funnel was extracted by 10-mL  $\text{CH}_2\text{Cl}_2$  three times, and all the organic phase was released to the flask. The combined organic phase was evaporated on a rotary evaporator. The dried flask was washed with 5 mL KOH- $\text{CH}_3\text{OH}$  solution (0.5 mol/L) three times, and all the extracted solution was taken into a test tube. Once 1–2 drops of Milli Q water were added, the solution was saponified in a 100 °C metal bath for 2 h. Then, the solution was extracted by 5 mL n-hexane three times to obtain neutral lipids. After that, the extracted hexane solution was evaporated by a rotary evaporator. The dried flask was washed with 1 mL n-hexane three times, and the solution was put into a 4 mL vial. The n-hexane was blow-dried with pure nitrogen ( $\text{N}_2$ ) gas, and then the neutral lipids were reacted with 100  $\mu\text{L}$  bis-trimethyl silyl tri fluoro acetamide (BSTFA) in 100  $\mu\text{L}$  acetonitrile at 100 °C for two hours. After blowing off BSTFA and acetonitrile by  $\text{N}_2$  gas, 50  $\mu\text{L}$  5 $\alpha$ -cholestane (2 mg/mL in hexane) internal standard and 100  $\mu\text{L}$  n-hexane were added in the vial for future analysis of neutral lipids.

Hydrochloric acid (HCl) solution (6 mol/L) was used to extract the fatty acids from the residual solution in the test tube until litmus paper revealed a pH value less than 2. The fatty acids were extracted with 5 mL n-hexane three times, and all the combined organic phases were transferred to a 50-mL pyriform flask and then evaporated. The flask was washed with  $3 \times 1$  mL  $\text{BF}_3$ -methanol, and the solution was transferred into a 20 mL test tube and then esterified at 100 °C for two hours to generate fatty acid methyl esters

(FAMES). Similar as neutral lipids, the FAMES in the test tube were extracted with 5 mL n-hexane three times. The n-hexane was removed by rotary evaporation, and the pyriform flask was washed with  $3 \times 1$  mL n-hexane. All the washed solution was transferred to a 4 mL vial. n-hexane in the vial was blow-dried with  $N_2$  gas, then 50  $\mu$ L internal standard nonadecanoic acid methyl ester (1 mg/mL in n-hexane) with 100  $\mu$ L n-hexane was added for the future analysis of fatty acids.

The lipids obtained through the above steps were defined as free lipids. After the extraction of free lipids, about 20 mL 0.5 mol/L KOH- $CH_3OH$  solution was added to the remaining sediment residue. The residue was heated at 100  $^{\circ}C$  for 2 h, and all other steps for separation and extraction were followed the same as for the free lipids. The lipids obtained from KOH- $CH_3OH$  solution treated residue were defined as bound lipids.

#### 2.4. Instrumental Analysis of Lipids

Fatty acids and neutral lipids were quantitatively examined by gas chromatography (GC: ECHROM A-90) connected with an automatic injector and flame ionization detector (FID) and qualitatively analyzed by gas chromatography-mass spectrometry (GC-MS: Agilent 7890A-5975C), based on the modified method of Yan et al. (2020) [2]. Different types of lipids were identified by molecular ion peaks and characteristic ion peaks. The chromatographic conditions of the GC-MS system were: DB-5MS column (30 m  $\times$  0.25 mm  $\times$  0.25  $\mu$ m); inlet temperature 280  $^{\circ}C$ ; ionization energy 70 eV; ion source temperature 230  $^{\circ}C$ ; injection volume 1  $\mu$ L; mass scan range 50–550 amu; helium was used as a carrier gas. The oven temperature gradient was the same for both GC and GC-MS (Figure 3). The total running time was 32 min.

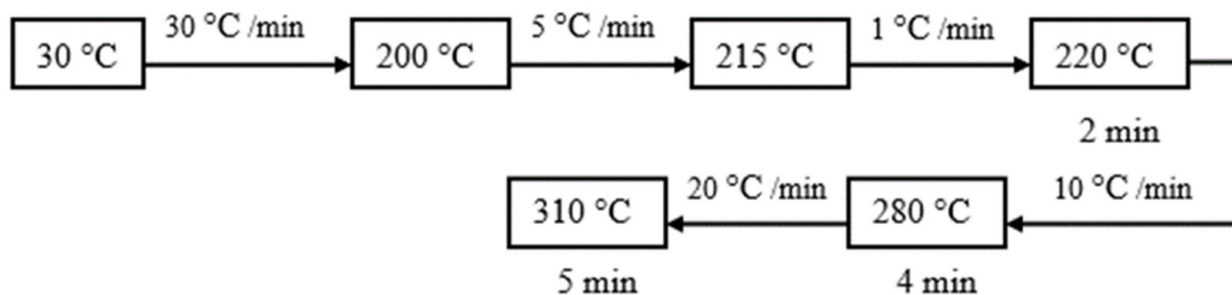


**Figure 3.** The oven temperature gradient for fatty acid methyl esters.

For neutral lipids, the column heating procedure was followed as shown in Figure 4. The total running time is 61 min. Nist 05 library was used to identify the fatty acids and the neutral lipids.

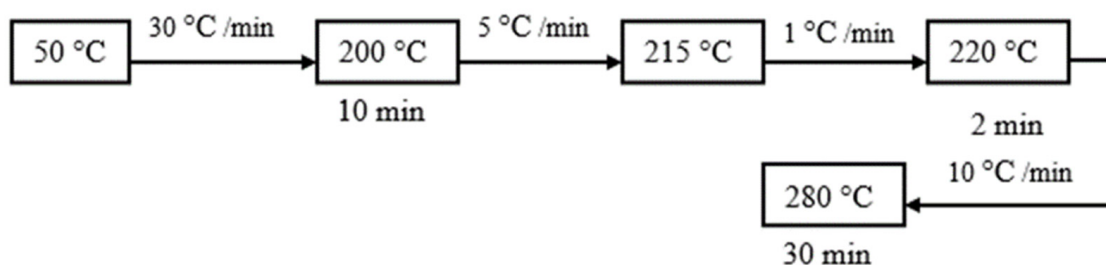


**Figure 4.** The oven temperature gradient for neutral lipids.

The chromatographic conditions of the GC system were: HP-5 column (30.0 m  $\times$  320  $\mu$ m  $\times$  0.25  $\mu$ m); hydrogen flame ionization detector (FID), inlet temperature was 310  $^{\circ}C$ ; injection volume was kept at 1  $\mu$ L; carrier gas was high purity  $N_2$ , carrier gas flow was selected 1 mL/min, airflow was controlled at 400 mL/min, and hydrogen flow was kept

at 40 mL/min. The concentration of each lipid species was determined by comparing the peak area of the internal standard with the peak area of an analyte in the GC spectrum.

### 2.5. Analysis of $\delta^{13}\text{C}$ of FAs

The FAMES were further analyzed to obtain the  $\delta^{13}\text{C}$  stable isotope ratio (IR) by gas chromatography isotope ratio mass spectrometer (GC-IRMS). The temperature gradient was elevated from 100 to 190 °C at 20 °C/min and increased to 230 °C at 1.5 °C/min, continued to 295 °C at 20 °C/min, and remained for 15 min. The column (HP-5, 50.0 m  $\times$  200  $\mu\text{m}$   $\times$  0.3  $\mu\text{m}$ ) was used to separate the FAMES. The injection volume was 2  $\mu\text{L}$ . The ignition temperature of furnace was set to 850 °C. The Vienna Pee Dee Belemnite (VPDB) was used as the standard for carbon isotopic ratio [36]. The  $\delta^{13}\text{C}$  of FAs were calculated based on the measured  $\delta^{13}\text{C}$  of the FAMES, the  $\delta^{13}\text{C}$  value of the methanol in  $\text{BF}_3$ -methanol reagent, and carbon number of the FAMES.

## 3. Results

### 3.1. Analysis of Lipid Biomarkers

In the sediment samples, 25 fatty acids were identified as saturated fatty acids (SFAs) (12:0, 14:0, 15:0, 16:0, 17:0, 18:0, 20:0); monounsaturated fatty acids (MUFAs) (12:1, 13:1, 14:1, 15:1, 16:1, 17:1, 18:1 $\omega$ 7, 18:1 $\omega$ 9, 20:1, 21:1, 22:1, 23:1) and the polyunsaturated fatty acids (PUFAs) (16: 3, 22:3, 22:4, 22:6, 23:2, 24:4), while 30 neutral lipids were determined in five classes as alkanes (14:0, 15:0, 16:0, 17:0, 18:0, 19:0, 20:0, 21:0, 22:0, 23:0, 24:0, 25:0, 26:0, 27:0), alkenes (olefins) (17:1, 22:1, 24:1, 26:1) including one phytene, normal fatty alcohols (alkanols) (12:0, 14:0, 15:0, 16:0, 17:0, 18:0, 19:0, 20:0), one phytol, and sterols (cholesterol, stigmasterol, sitosterol) in free and bound forms.

### 3.2. Composition and Vertical Distribution of Lipids

Regarding observed data for fatty acids (Figure 5), most of them in the hadal sediment from station D113 were in bound form with the maximum concentrations of 16:0 (163.88  $\mu\text{g/g}$ ) and 18:0 (132.02  $\mu\text{g/g}$ ). Fatty acid 24:4 was also in a higher concentration of 70.62  $\mu\text{g/g}$  in the hadal sediment. The concentrations of remaining fatty acids were all below 25  $\mu\text{g/g}$ . In vertical distributions, SFAs were the main components in surface sediments, representing 78% of total fatty acids. MUFAs were also higher in the surface layer, and the concentration was in a decreasing trend and was 17% in total FAs. In contrast, the PUFAs were higher in the 2 and 8 cm layers and were only 5% in total concentration. In the abyssal sediment from station S01, the highest concentrations of fatty acids were also observed in the surface layer. The total concentration of fatty acids was 96.72  $\mu\text{g/g}$ , with the highest concentrations of 16:0 and 18:0, followed by 22:4 and 22:6. MUFAs were the main components in the sediment from station S01, accounted for 50% of total fatty acids, followed by PUFAs (29%). The SFAs occupied 21% of total fatty acids, while fatty acid 18:1 $\omega$ 7 was observed in a high concentration of 9.07  $\mu\text{g/g}$ . Most of the fatty acids in this abyssal sediment were in free form, but the high concentration fatty acids were in bound form. From abyssal to hadal sediments of the north Yap Trench, the concentrations and compositions of fatty acids changed significantly. In the hadal sediment, the SFAs were the major components, but in the abyssal sediment, the MUFAs were the main components. The concentration of PUFAs were higher than the SFAs in the abyssal sediments.

According to the distributions of neutral lipids (Figure 6), the carbon number of alkanes was between C14-C27. The alkanes in the sediments of both stations had an even carbon advantage with a higher concentration of even carbon alkanes. Regarding the hadal sediment core from station D113, alkanes were observed with higher concentrations in the surface sediment layer, up to 15.74  $\mu\text{g/g}$  in free and bound form. The concentrations of sterols and alkanols (fatty alcohols) were higher and were mostly in bound form. In general, their concentrations decreased with sediment depth. However, the higher concentration of alkanol species were C19 and C17, at 18.67 and 13.94  $\mu\text{g/g}$  in free form. In the bound form of the sediment from station D113, the higher concentration species of alkanols were

C19 and C17, with 10.04 and 6.93  $\mu\text{g/g}$ , respectively. Most of the fatty alcohols were in free form. However, the alkenes (olefins) and phytol concentrations were low. The total concentration of alkenes were 24.70 and 2.76  $\mu\text{g/g}$  in free and bound form, and the concentration of phytol were 26.39 and 6.12  $\mu\text{g/g}$  in free and bound forms, respectively. The highest alkane concentrations in the abyssal sediment core were observed in the surface layer up to 71.74  $\mu\text{g/g}$  (C14) in bound form, and the remaining alkane concentrations were below 7.0  $\mu\text{g/g}$  and were mainly in bound form. Generally, concentrations of alkanols in sediment core from station S01 were higher in bound form, and the species with higher concentrations were C19 and C20, as 19.64 and 7.74  $\mu\text{g/g}$ . Concentrations of free alkanols were less than those of bound alkanols. The distribution patterns of sterols in the sediment samples from both stations were almost similar. The total concentration of bound sterols in the sediment from station D113 was observed to be higher in the surface layer as 27.13  $\mu\text{g/g}$ , and the concentration decreased with depth. Whereas in station S01, bound sterols were also higher in the surface sediment layer, and the concentrations decreased dramatically in the 2 cm layer. Below this layer, their concentrations changed a little with depth. The cholesterol concentration increased in both free and bound forms with depth. Its highest concentration was observed 27.13  $\mu\text{g/g}$  in the surface layer and was mostly in bound form, and the concentration decreased with depth. However, the total concentration of neutral lipids of abyssal sediment is higher, up to 517.05  $\mu\text{g/g}$ , compared to the hadal sediment 345.85  $\mu\text{g/g}$ .

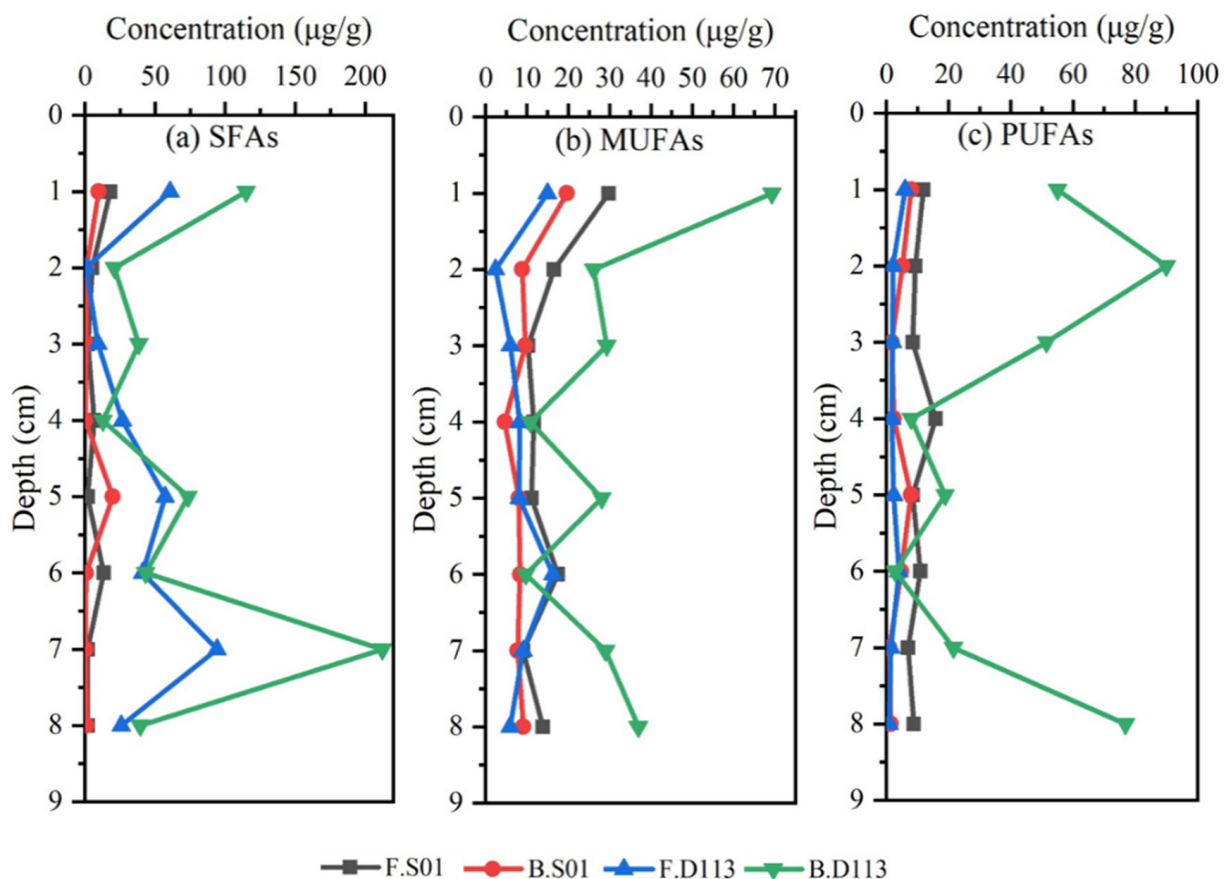


**Figure 5.** Comparison of concentrations of FAs in the two sediment samples. Where panel (a) represents the concentrations of SFAs, panel (b) represents the MUFAs, and panel (c) represents the PUFAs in free and bound forms of the two stations. F.S01 and F.D113 represent free FAs and B.S01 and B.D113 represent bound FAs in the two sediment samples.

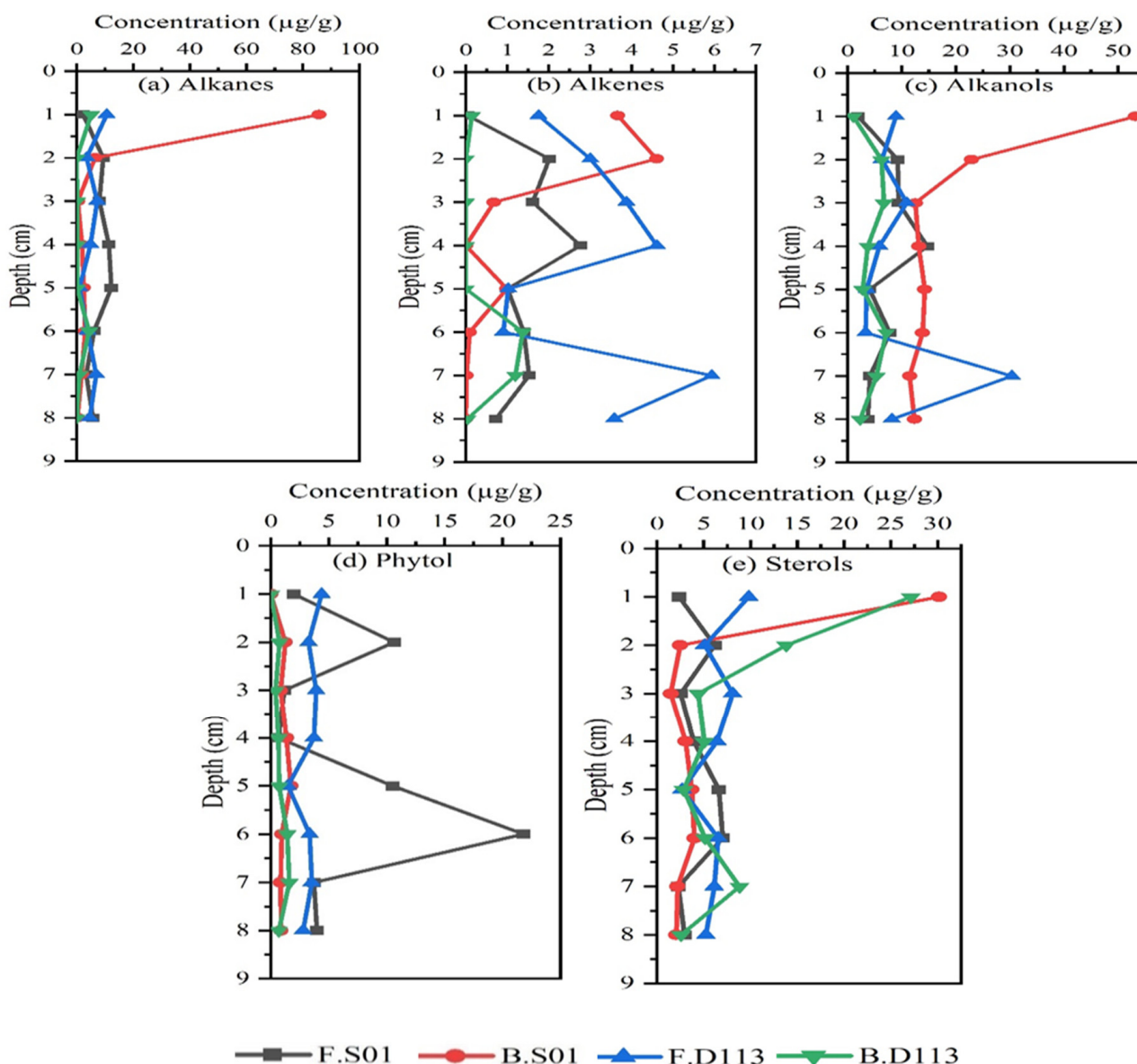


**Figure 6.** Vertical distribution profiles of neutral lipids in total concentrations. Where F.S01 and F.D113 represent free neutral lipids and B.S01 and B.D113 represent bound neutral lipids in the two sediment samples. Panel (a) shows the total concentrations of alkanes, panel (b) shows the concentrations of alkenes, panel (c) shows the total concentrations of alkanols, panel (d) shows the concentration of phytol, and panel (e) shows the total concentrations of sterols.

Whereas the  $\delta^{13}\text{C}$  values of FAs from the abyssal and the hadal sediment cores (Figure 7) were observed to be highly depleted regarding free and bound forms. The  $\delta^{13}\text{C}$  ratios of FAs from the hadal sediment core ranged from  $-20.83$  to  $-40.98\%$  in free form, while in bound form ranged from  $-20.3$  to  $-52.63\%$ . For the abyssal sediment, the  $\delta^{13}\text{C}$  values of FAs ranged from  $-12.03$  to  $-48.76\%$  in free form and  $-10.65$  to  $-54.61\%$  in bound form.

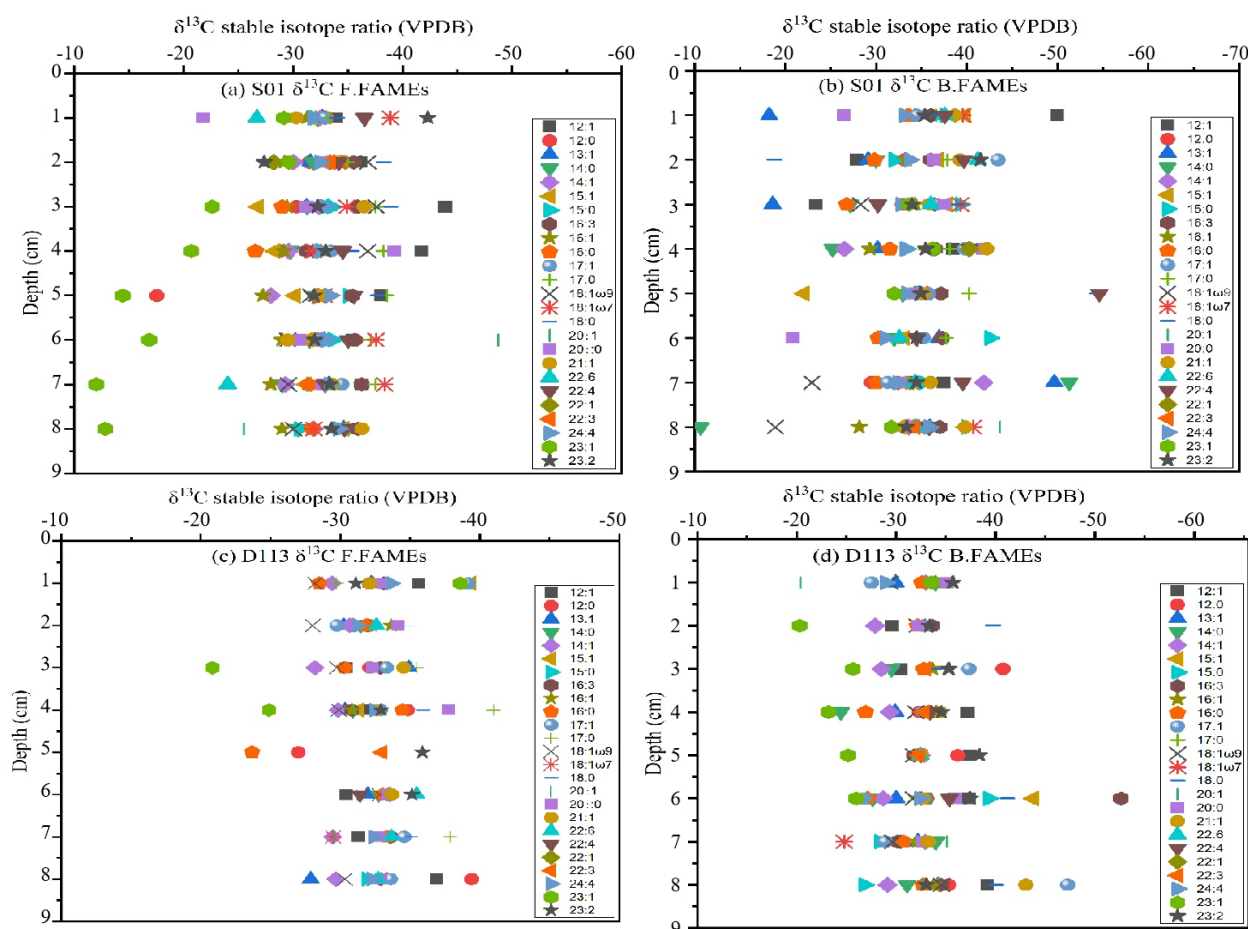


**Figure 7.** The  $\delta^{13}\text{C}$  values of FAs from sediment samples of the north Yap Trench. Panels (a,b) represent the  $\delta^{13}\text{C}$  values of free and bound FAs in the sediment sample from station S01, and panels (c,d) represent the  $\delta^{13}\text{C}$  values of free and bound FAs in the sediment sample from station D113.

#### 4. Discussion

##### 4.1. Lipid Biomarkers in the Marine Environment

Microbial degradation of organic matter throughout the sedimentary column affects the data of various isotopes and biomarkers used to interpret paleo-environment records [37–39]. The complex geochemistry of organic matter in the ocean environment and the high rate of inputs from exotic sources alter the physical, chemical, and biological settings of seabed, with severe consequences for ecosystem functions [40–43]. Miscellaneous organic matter can harm the marine environment. In some cases, high organic matter inputs from different sources can increase the productivity of the marine environment [44]. The degradation of organic matter, deposition, and rock formation gives the sources of origin and past environmental conditions in sediments [45–48]. The sources and biogeochemical processes of organic matter strongly influence the species, concentrations, distributions, and  $\delta^{13}\text{C}$  values of lipid biomarkers in marine sediment.

The V-shaped topographical feature of the Yap Trench facilitates the accumulation of organic matter to its bottom, resulting in higher lipid concentrations in the hadal sediment. The sediments in the offshore areas tend to have the highest concentrations of 16:0 and 16:1, while a higher concentration of 18:0 is an important feature of the Yap Trench sediments. Previous research showed that the concentrations of lipids in open sea area sediments was lower than those in the Yap Trench sediments. For example, the concentrations of lipids in the surface sediments of the Yellow Sea were between 20.65 and 44.72  $\mu\text{g/g}$  [49] and ranged from 11.58 to 31.58  $\mu\text{g/g}$  in the muddy areas of the East China Sea [50,51]. In the sediment of the South China Sea, concentrations of lipids varied from 7.85 to 47.37  $\mu\text{g/g}$  [43]. The

concentration of lipids from the surface sediments of the Campos Basin (2500–3000 m) was as low as 4.84  $\mu\text{g/g}$  [52]. The existence of submarine hydrothermal fluid also has a significant effect on the concentration of lipid biomarkers [49,52]. The total amount of fatty acids in this study was significantly higher than those in offshore sediments. In hadal sediments from station D113, the concentration was above 300  $\mu\text{g/g}$ , reflecting funnel effect of the Yap Trench on organic matter deposition.

#### 4.2. Sources of Fatty Acids

According to the sources of fatty acids, even carbon SFAs with carbon numbers less than 20, such as (12:0, 14:0, 16:0, 18:0, and 20:0) and MUFA 18:1 $\omega$ 9, are considered of mixed origin (land and sea sources), and PUFAs (16:3, 22:3, 22:4, 22:6, 23:2, 24:4) and MUFA 16:1 can be from aquatic phytoplankton and also from land sources. PUFA 22:6 is from the intracellular origin [53]. However, the odd carbon number fatty acids (15:0, 17:0) and MUFA 18:1 $\omega$ 7 are mostly considered from bacteria [54]. The bacterial fatty acid 18:1 $\omega$ 7 is usually associated with sulfur-oxidizing bacteria, found mainly in submarine hydrothermal areas and seafloor hydrothermal fluids [55,56]. The existence of these fatty acids in the abyssal and hadal sediment from the north Yap Trench indicates a complex source of organic matter in the marine trench system.

The morphological distribution of fatty acids in sediments varies in different places. For example, in the Changjiang Estuary, the bound FAs in surface sediments were more significant than in free form [57]. The main forms of fatty acids in the South China Sea sediment samples and the Black Sea were in free form [54,55]. In general, the degradation of bound fatty acids (BFAs) in sediments ought to be slower than that of free fatty acids (FFAs) because of their lower bioavailability [56]. As the deposit deepens, the fraction of FFAs in the total fatty acids should show a reducing trend. However, the fraction of free fatty acids in the abyssal and hadal sediment of the north Yap Trench was higher than that of BFAs. A possible explanation may attribute to the funnel effect. The V-shape topography of the trench promoted faster deposit and burial of organic matter in the sediment. The formation of anoxic environment in deeper sediment slowed down the degradation of organic matter, and then a large amount of free fatty acids were preserved in the abyssal and hadal zone of the trench [58]. On the other side, the north Yap trench is a junction of three plates (the Pacific Plate, the Philippine Plate, and the Caroline Plate [2]). Complex water current and active geological activities in the study area was not conducive to the adsorption of organic matters by sediments, causing the decrease of fraction of BFAs.

#### 4.3. Sources of Neutral Lipids

Due to the influence of deep-sea hydrothermal fluid, a high amount of organic matter accumulates in sediments. Alkanes as biomarkers can imitate the sources of organic matter [59]. Alkanes with a carbon number ( $C_n$ ) < 21 are mainly considered the derivatives of bacteria, algae, and marine plankton [60]. Higher carbon alkanes ( $C_n > 25$ ) are commonly thought to have sources of terrestrial plants and animals [61]. According to the distribution of stigmaterol (a typical lipid of terrestrial plants) in the two sediment samples, the content of the land source was significantly higher, indicating that the sterols are mainly from terrestrial input [62]. Higher animals usually contain cholesterol. As the Yap Trench belongs to a deep ocean trench system, it is difficult to produce large amounts of cholesterol, and the input of animal organic matter was much less than that of plants, causing lower concentrations of cholesterol in the sediment samples [63]. Terrestrial sterols can also reach the abyssal and hadal sediments and are partially retained there. The carbon chain of alkanols was less than 20, which is mainly considered from microbial and other marine sources [58]. As phytol is primarily a derivative of phytoplankton, the morphological distribution pattern of phytol in the sediment of station S01 was observed to be similar as in offshore sediments and was mostly in the bound form [63]. Whereas five members of alkene from 17:1 to 26:1, including one phytene can initiate from the microbial conversion of

the corresponding n-alkanes or direct inputs from micro-organisms, alkenes are sometimes abundant and comprise the compounds derivative of diatomaceous algae [64].

#### 4.4. Characteristic Preference Index of Lipid Biomarkers

According to the characteristic preference index (CPI) of fatty acids (Table 2), even carbon compounds take precedence if the value is greater than 1. In our study, except for individual cases, the CPI values are more than 1 in all depths of the two sediment samples in both free and bound forms, with the highest value 128.40, indicating a significant even carbon advantage in FAs. In fact, most of the FAs generated in eukaryotes are even carbon numbers. Odd carbon number FAs are converted from even carbon number FAs. It is reasonable to find more even carbon number FAs in the sediment samples. C18:1 $\omega$ 7/C18:1 $\omega$ 9 ratios varied from 0.11 to 4.92, providing evidence of bacterial sources [65]. The CPI of C16:1/C16:0 ranged from 0.49 to 3.03 in free and bound forms in the two sediment samples. The C16:1/C16:0 ratio was used to discriminate contributions of diatom and dinoflagellate in marine sediment [66]. The presence of diatom-derived organic matter was suggested by a C16:1/C16:0 ratio greater than 1.6. In this study, most of the ratios were smaller than 1.6. Only the 3 cm layer of the sediment from station S01 has a C16:1/C16:0 value of 2.4 in free form, and its surface layer has a value of 1.90 in bound form, indicating less contribution of diatoms for organic matter in the sediment samples. However, plenty of diatom microfossils were found in the sediment from station D113, showing that diatom was an important source of organic matter in the sediment [3]. It is possible that because unsaturated fatty acids are more susceptible to biological and chemical breakdown during sedimentation, the C16:1/C16:0 ratio is frequently much below 1 [67].

**Table 2.** CPI values of fatty acids from the sediments of the Yap Trench.

	CPI Values of FFAs						CPI Values of BFAs				
	Depth/ (cm)	(Odd/ Even)	(Even/ Odd)	C16:0/ C18:0	C16:1/ C16:0	C18:1 $\omega$ 7/ 18:1 $\omega$ 9	(Odd/ Even)	(Even/ Odd)	C16:0/ C18:0	C16:1/ C16:0	C18:1 $\omega$ 7/ 18:1 $\omega$ 9
D113	1	0.0	56.12	0.63	0.01	4.92	0.03	33.63	0.89	0.02	0.72
	2	8.81	0.11	0.00	0.00	1.12	0.03	29.03	1.29	0.02	0.37
	3	0.14	7.10	1.57	0.02	0.91	0.02	35.40	1.31	0.02	0.26
	4	0.04	24.26	1.25	0.01	1.51	0.04	20.31	1.25	0.02	0.78
	5	0.03	33.19	1.08	0.01	1.17	0.05	18.57	0.84	0.01	0.46
	6	0.02	43.73	0.64	0.01	3.48	0.01	80.65	0.48	0.01	4.81
	7	0.02	41.76	1.25	0.00	1.00	0.01	86.43	1.23	0.01	0.41
	8	0.04	24.52	1.15	0.01	1.00	0.02	41.50	1.03	0.02	0.26
S01	1	0.04	24.91	0.66	0.46	2.83	0.10	10.33	0.12	1.89	0.37
	2	0.01	62.08	3.03	0.71	0.23	0.68	1.47	0.00	0.00	0.36
	3	0.08	11.11	0.64	2.43	0.00	0.66	1.51	0.00	0.00	0.55
	4	0.06	14.37	1.00	0.71	0.17	0.00	0.00	0.00	0.00	0.82
	5	0.12	8.132	0.00	0.00	0.16	0.03	32.61	0.78	0.13	0.00
	6	0.01	128.39	1.01	0.39	0.08	0.19	5.41	0.00	0.00	0.11
	7	0.72	1.38	0.00	0.00	0.21	0.11	9.11	0.00	0.00	0.88
	8	0.09	10.89	0.00	0.00	0.35	0.52	1.92	0.00	0.00	0.69

According to CPI values of neutral lipids (Table 3), the CPI1 (used for marine and aquatic sources) and CPI2 (used for terrestrial sources) values are lower than 1 in all the sediment layers of the sediment sample from station D113, with an obvious even carbon advantage. The short-chain alkanes in the sediment of station S01 have an obvious even carbon advantage; and long-chain alkanes have a distinct odd carbon advantage, having CPI2 values ranging from 0.87 to 2.29. In addition, the ratios of heavy to light hydrocarbons (H/L) were observed to be less than 1, representing that alkanes are mainly low-level biological inputs, such as bacteria and algae [68]. In the sediment sample from station D113, the terrestrial/aquatic lipid ratio (TAR) was primarily negligible. In the sediment sample from station S01, TAR values in free form varied from 0.18 to 9.87, and in bound form, only

1 and 2 cm layers had values of 0.39 and 4.60, respectively. In general, typical terrestrial sedimentation has a TAR value of less than 1.1. Thus, the sediment in station D113 should be of marine origin, and the sediments in S01 station have mixed terrestrial and marine origin [69].

**Table 3.** CPI values of Alkanes from sediments of the Yap Trench.

	Depth(cm)	CPI Values of Free Alkanes				CPI Values of Bound Alkanes			
		H/L	TAR	CPI <sub>1</sub>	CPI <sub>2</sub>	H/L	TAR	CPI <sub>1</sub>	CPI <sub>2</sub>
D113	1	0.90	0.98	0.70	0.76	12.0	0.0	0.0	1.52
	2	0.18	0.0	0.24	0.0	0.0	0.0	0.0	0.0
	3	0.24	0.0	0.94	0.0	2.43	0.0	0.0	0.0
	4	0.34	0.0	0.74	0.0	0.0	0.0	0.0	0.0
	5	0.0	0.0	0.0	0.0	0.0	0.0	0.0	0.0
	6	0.29	0.05	0.58	0.06	0.2	0.0	0.51	0.0
	7	0.28	0.0	0.89	0.0	3.01	0.0	0.0	0.0
	8	0.21	0.0	0.93	0.0	0.0	0.0	0.0	0.0
S01	1	0.05	0.36	0.08	0.98	0.0	0.39	0.10	1.30
	2	0.65	9.87	0.02	1.80	0.19	4.60	0.0	0.0
	3	0.98	0.37	0.3	1.42	0.20	0.0	0.0	0.0
	4	1.07	0.18	0.22	1.22	0.89	0.0	0.0	1.31
	5	1.21	1.33	0.26	1.35	0.62	0.0	0.1	3.20
	6	1.74	7.53	0.07	2.29	4.88	0.0	0.0	3.68
	7	1.72	0.0	0.21	1.09	4.37	0.0	0.0	0.71
	8	0.91	0.27	0.27	0.87	0.0	0.0	0.0	0.0

Note: H/L = HMW (C25 – C27)/LMW (C14 – C24); TAR = C27/ (C15 + C17 + C19); CPI<sub>1</sub> =  $\frac{\sum(C15 - C21) \text{ odd}}{\sum(C14 - C20) \text{ even}}$ ; CPI<sub>2</sub> = (C25 + C27)/C26.

#### 4.5. Tracking the Sources of FAs According to the $\delta^{13}\text{C}$ Stable Isotope Values

According to the sources of  $^{13}\text{C}$  stable isotopes, the strongly depleted  $\delta^{13}\text{C}$  values such as  $-48$  to  $-54\text{‰}$  indicated the existence of methane-related microorganisms [70]. It is conceivable that some microbes in the research area are utilizing methane ( $\text{CH}_4$ ) from hydrothermal vents, such as methanogen microbes, to produce organic carbon with depleted  $\delta^{13}\text{C}$  values [58]. The most depleted values of  $\delta^{13}\text{C}$  from the sediment cores also revealed the presence of anaerobic methane-oxidizing archaea in the hydrothermal site of the trench. From the study by Fu et al. [71], the  $\delta^{13}\text{C}$  values of methanotrophic symbiotic microorganisms in mussels ranged from  $-39.6$  to  $-45.4\text{‰}$ . On the other side, the depleted  $\delta^{13}\text{C}$  values are considered definite for recent and ancient methane vent activities [21,72] and possibly from methane seeps and mud volcanoes. Lipid biomarkers give the evidence that archaea can be involved in reducing methane and possibly proficient in consuming methane as a sole carbon source in anaerobic conditions. The study about microbial populations in the Yap Trench [71] showed that the *Proteobacteria* and *Thaumarchaeota* were dominated microbes controlling the major metabolic processes. They also discovered different kinds of ammonia-oxidizing archaea (AOA), ammonia-oxidizing bacteria (AOB), and sulfate-reducing bacteria (SRB). The FAs (16:3, 18:0, 12:0, 12:1, 16:0) in the sediment from station D113 and FAs (18:0, 14:0, 12:1, 13:1, 17:1, 15:0) in the sediment from station S01 with remarkable depleted  $\delta^{13}\text{C}$  values show that these organisms can adapt deeper depths to survive by adjusting their membrane composition. It would be implemented where methanogenic archaea are operative as opposite in a syntrophic confederation with sulfate-reducing bacteria (SRB) [70,73].

## 5. Conclusions

The distributions and compositions of the lipid biomarkers, including fatty acids, n-alkanes, n-alkanols, alkenes, phytol, and sterols in the sediment from the abyss and hadal zone of the north Yap Trench, were determined. The results revealed that: (1) Algae and bacteria were the primary sources of organic matter in the sediments, and marine plankton

with terrestrial sources have relatively limited contribution. (2) The variations of lipid compositions and distributions in the surface sediments of the two samples may have been brought about by differential lipid biomarker degradation, which led to lipid biomarkers contributing more to the organic matter in the sediments. (3) The extremely depleted  $\delta^{13}\text{C}$  values might be from methane-related microorganisms, including methanogenic microbes. (4) The  $\delta^{13}\text{C}$  values also provided evidence of the existence of sulfur-reducing bacteria in aerobic and anaerobic oxidation and archaea in the study area. (5) The funnel effect of the V-shape geological structure of the trench promoted deposition and burial of organic matter and caused a high fraction of free fatty acids in the abyssal and hadal sediments. This study provides essential information on the organic materials of abyssal and hadal environments and is helpful for a deeper understanding of organic carbon in the marine trench system. Due to the limited ability of the “Jiaolong” manned submersible, the sediment from deeper depths is unavailable. A more advanced submersible is necessary to conduct the investigation in deeper depth to understand the whole trench.

**Author Contributions:** Methodology, C.S., A.H.K. and H.D.; formal analysis, A.H.K. and H.D.; resources, C.S.; writing—original draft preparation, A.H.K. and H.D.; writing—review and editing, Gui-Peng Yang; supervision, C.S., G.-P.Y. and H.D.; project administration, C.S. and H.D.; funding acquisition, C.S., G.-P.Y. and H.D. All authors have read and agreed to the published version of the manuscript.

**Funding:** This research was funded by the Natural National Science Foundation of China, grant number 42076040; 41776177; and 41676067; and the 111 Project: grant number B13030.

**Conflicts of Interest:** The authors declare no conflict of interest.

## References

1. Taira, K.; Yanagimoto, D.; Kitagawa, S. Deep CTD Casts in the Challenger Deep, Mariana Trench. *J. Oceanogr.* **2005**, *61*, 447–454. [[CrossRef](#)]
2. Yan, Y.; Sun, C.; Huang, Y.; Cao, W.; Jiang, F.; Yang, G.; Ding, H. Distribution Characteristics of Lipids in Hadal Sediment in the Yap Trench. *J. Oceanol. Limnol.* **2020**, *38*, 634–649. [[CrossRef](#)]
3. Huang, Y.; Sun, C.; Yang, G.; Yue, X.; Jiang, F.; Cao, W.; Yin, X.; Guo, C.; Niu, J.; Ding, H. Geochemical Characteristics of Hadal Sediment in the Northern Yap Trench. *J. Oceanol. Limnol.* **2020**, *38*, 650–664. [[CrossRef](#)]
4. Li, Z.; Sun, Y.; Nie, X. Biomarkers as a Soil Organic Carbon Tracer of Sediment: Recent Advances and Challenges. *Earth-Sci. Rev.* **2020**, *208*, 103277. [[CrossRef](#)]
5. Luo, M.; Gieskes, J.; Chen, L.; Shi, X.; Chen, D. Provenances, Distribution, and Accumulation of Organic Matter in the Southern Mariana Trench Rim and Slope: Implication for Carbon Cycle and Burial in Hadal Trenches. *Mar. Geol.* **2017**, *386*, 98–106. [[CrossRef](#)]
6. Luo, M.; Glud, R.N.; Pan, B.; Wenzhöfer, F.; Xu, Y.; Lin, G.; Chen, D. Benthic Carbon Mineralization in Hadal Trenches: Insights from in Situ Determination of Benthic Oxygen Consumption. *Geophys. Res. Lett.* **2018**, *45*, 2752–2760. [[CrossRef](#)]
7. Gallo, N.D.; Cameron, J.; Hardy, K.; Fryer, P.; Bartlett, D.H.; Levin, L.A. Submersible-and Lander-Observed Community Patterns in the Mariana and New Britain Trenches: Influence of Productivity and Depth on Epibenthic and Scavenging Communities. *Deep Sea Res. Part I Oceanogr. Res. Pap.* **2015**, *99*, 119–133. [[CrossRef](#)]
8. Glud, R.N.; Wenzhöfer, F.; Middelboe, M.; Oguri, K.; Turnewitsch, R.; Canfield, D.E.; Kitazato, H. High Rates of Microbial Carbon Turnover in Sediments in the Deepest Oceanic Trench on Earth. *Nat. Geosci.* **2013**, *6*, 284–288. [[CrossRef](#)]
9. Bao, R.; Strasser, M.; McNichol, A.P.; Haghypour, N.; McIntyre, C.; Wefer, G.; Eglinton, T.I. Tectonically-Trigged Sediment and Carbon Export to the Hadal Zone. *Nat. Commun.* **2018**, *9*, 1–8. [[CrossRef](#)]
10. Danovaro, R.; Della Croce, N.; Dell’Anno, A.; Pusceddu, A. A Depocenter of Organic Matter at 7800 m Depth in the SE Pacific Ocean. *Deep Sea Res. Part I Oceanogr. Res. Pap.* **2003**, *50*, 1411–1420. [[CrossRef](#)]
11. Leduc, D.; Rowden, A.A. Nematode Communities in Sediments of the Kermadec Trench, Southwest Pacific Ocean. *Deep Sea Res. Part I Oceanogr. Res. Pap.* **2018**, *134*, 23–31. [[CrossRef](#)]
12. Li, D.; Zhao, J.; Yao, P.; Liu, C.; Sun, C.; Chen, J.; Pan, J.; Han, Z.; Hu, J. Spatial Heterogeneity of Organic Carbon Cycling in Sediments of the Northern Yap Trench: Implications for Organic Carbon Burial. *Mar. Chem.* **2020**, *223*, 103813. [[CrossRef](#)]
13. Longhurst, A.; Sathyendranath, S.; Platt, T.; Caverhill, C. An Estimate of Global Primary Production in the Ocean from Satellite Radiometer Data. *J. Plankton Res.* **1995**, *17*, 1245–1271. [[CrossRef](#)]
14. Itou, M.; Matsumura, I.; Noriki, S. A Large Flux of Particulate Matter in the Deep Japan Trench Observed Just after the 1994 Sanriku-Oki Earthquake. *Deep Sea Res. Part I Oceanogr. Res. Pap.* **2000**, *47*, 1987–1998. [[CrossRef](#)]

15. Turnewitsch, R.; Falahat, S.; Stehlikova, J.; Oguri, K.; Glud, R.N.; Middelboe, M.; Kitazato, H.; Wenzhöfer, F.; Ando, K.; Fujio, S. Recent Sediment Dynamics in Hadal Trenches: Evidence for the Influence of Higher-Frequency (Tidal, near-Inertial) Fluid Dynamics. *Deep Sea Res. Part I Oceanogr. Res. Pap.* **2014**, *90*, 125–138. [[CrossRef](#)]
16. Nunoura, T.; Takaki, Y.; Hirai, M.; Shimamura, S.; Makabe, A.; Koide, O.; Kikuchi, T.; Miyazaki, J.; Koba, K.; Yoshida, N. Hadal Biosphere: Insight into the Microbial Ecosystem in the Deepest Ocean on Earth. *Proc. Natl. Acad. Sci. USA* **2015**, *112*, E1230–E1236. [[CrossRef](#)] [[PubMed](#)]
17. Oguri, K.; Kawamura, K.; Sakaguchi, A.; Toyofuku, T.; Kasaya, T.; Murayama, M.; Fujikura, K.; Glud, R.N.; Kitazato, H. Hadal Disturbance in the Japan Trench Induced by the 2011 Tohoku–Oki Earthquake. *Sci. Rep.* **2013**, *3*, 1915. [[CrossRef](#)]
18. Jamieson, A.J.; Fujii, T.; Mayor, D.J.; Solan, M.; Priede, I.G. Hadal Trenches: The Ecology of the Deepest Places on Earth. *Trends Ecol. Evol.* **2010**, *25*, 190–197. [[CrossRef](#)]
19. Rex, M.A.; Etter, R.J.; Morris, J.S.; Crouse, J.; McClain, C.R.; Johnson, N.A.; Stuart, C.T.; Deming, J.W.; Thies, R.; Avery, R. Global Bathymetric Patterns of Standing Stock and Body Size in the Deep-Sea Benthos. *Mar. Ecol. Prog. Ser.* **2006**, *317*, 1–8. [[CrossRef](#)]
20. Wang, L.; MacLennan, S.A.; Cheng, F. From a Proximal-Deposition-Dominated Basin Sink to a Significant Sediment Source to the Chinese Loess Plateau: Insight from the Quantitative Provenance Analysis on the Cenozoic Sediments in the Qaidam Basin, Northern Tibetan Plateau. *Palaeogeogr. Palaeoclimatol. Palaeoecol.* **2020**, *556*, 109883. [[CrossRef](#)]
21. Alba-González, P.; Álvarez-Salgado, X.A.; Cobelo-García, A.; Kaal, J.; Teira, E. Faeces of Marine Birds and Mammals as Substrates for Microbial Plankton Communities. *Mar. Environ. Res.* **2022**, *174*, 105560. [[CrossRef](#)]
22. Koszelnik, P.; Gruca-Rokosz, R.; Bartoszek, L. An Isotopic Model for the Origin of Autochthonous Organic Matter Contained in the Bottom Sediments of a Reservoir. *Int. J. Sediment Res.* **2018**, *33*, 285–293. [[CrossRef](#)]
23. Abdel-Wahab, M.A.; El-Samawaty, A.E.R.M.A.; Elgorban, A.M.; Bahkali, A.H. Fatty Acid Production of Thraustochytrids from Saudi Arabian Mangroves. *Saudi J. Biol. Sci.* **2021**, *28*, 855–864. [[CrossRef](#)] [[PubMed](#)]
24. Guan, H.; Chen, L.; Luo, M.; Liu, L.; Mao, S.; Ge, H.; Zhang, M.; Fang, J.; Chen, D. Composition and Origin of Lipid Biomarkers in the Surface Sediments from the Southern Challenger Deep, Mariana Trench. *Geosci. Front.* **2019**, *10*, 351–360. [[CrossRef](#)]
25. Tao, K.; Xu, Y.; Wang, Y.; Wang, Y.; He, D. Source, Sink and Preservation of Organic Matter from a Machine Learning Approach of Polar Lipid Tracers in Sediments and Soils from the Yellow River and Bohai Sea, Eastern China. *Chem. Geol.* **2021**, *582*, 120441. [[CrossRef](#)]
26. Lee, S.-M. Deformation from the Convergence of Oceanic Lithosphere into Yap Trench and Its Implications for Early-Stage Subduction. *J. Geodyn.* **2004**, *37*, 83–102. [[CrossRef](#)]
27. Ohara, Y.; Reagan, M.K.; Fujikura, K.; Watanabe, H.; Michibayashi, K.; Ishii, T.; Stern, R.J.; Pujana, I.; Martinez, F.; Girard, G. A Serpentine-Hosted Ecosystem in the Southern Mariana Forearc. *Proc. Natl. Acad. Sci. USA* **2012**, *109*, 2831–2835. [[CrossRef](#)]
28. Fujiwara, T.; Tamura, C.; Nishizawa, A.; Fujioka, K.; Kobayashi, K.; Iwabuchi, Y. Morphology and Tectonics of the Yap Trench. *Mar. Geophys. Res.* **2000**, *21*, 69–86. [[CrossRef](#)]
29. Shiraki, K. Metamorphic Basement Rocks of Yap Islands, Western Pacific: Possible Oceanic Crust beneath an Island Arc. *Earth Planet. Sci. Lett.* **1971**, *13*, 167–174. [[CrossRef](#)]
30. Hawkins, J.; Batiza, R. Metamorphic Rocks of the Yap Arc-Trench System. *Earth Planet. Sci. Lett.* **1977**, *37*, 216–229. [[CrossRef](#)]
31. McCabe, R.; Uyeda, S. Hypothetical Model for the Bending of the Mariana Arc. *Wash. DC Am. Geophys. Union Geophys. Monogr. Ser.* **1983**, *27*, 281–293.
32. Song, Y.; Ma, X.; Zhang, G.; Liu, X.; Luan, Z.; Dong, D.; Yan, J. Heat Flow In-Situ Measurement at Yap Trench of the Western Pacific. *Mar. Geol. Quat. Geol.* **2016**, *36*, 51–56.
33. Yang, Y.; Wu, S.; Gao, J.; Tian, L.; Yang, J.; Xu, Y. Geology of the Yap Trench: New Observations from a Transect near 10° N from Manned Submersible Jiaolong. *Int. Geol. Rev.* **2018**, *60*, 1941–1953. [[CrossRef](#)]
34. Wenzhöfer, F.; Oguri, K.; Middelboe, M.; Turnewitsch, R.; Toyofuku, T.; Kitazato, H.; Glud, R.N. Benthic Carbon Mineralization in Hadal Trenches: Assessment by in Situ O<sub>2</sub> Microprofile Measurements. *Deep Sea Res. Part I Oceanogr. Res. Pap.* **2016**, *116*, 276–286. [[CrossRef](#)]
35. Liu, Y.; Liu, X.; Lv, X.; Cao, W.; Sun, C.; Lu, J.; Wang, C.; Lu, B.; Yang, J. Watermass Properties and Deep Currents in the Northern Yap Trench Observed by the Submersible Jiaolong System. *Deep Sea Res. Part I Oceanogr. Res. Pap.* **2018**, *139*, 27–42. [[CrossRef](#)]
36. Coplen, T.B. Discontinuance of SMOW and PDB. *Nature* **1995**, *375*, 285. [[CrossRef](#)]
37. Holtvoeth, J.; Whiteside, J.H.; Engels, S.; Freitas, F.S.; Grice, K.; Greenwood, P.; Johnson, S.; Kendall, I.; Lengger, S.K.; Lücke, A.; et al. The Paleolimnologist’s Guide to Compound-Specific Stable Isotope Analysis—An Introduction to Principles and Applications of CSIA for Quaternary Lake Sediments. *Quat. Sci. Rev.* **2019**, *207*, 101–133. [[CrossRef](#)]
38. Wehrmann, L.M.; Arndt, S.; März, C.; Ferdelman, T.G.; Brunner, B. The Evolution of Early Diagenetic Signals in Bering Sea Subseafloor Sediments in Response to Varying Organic Carbon Deposition over the Last 4.3 Ma. *Geochim. Cosmochim. Acta* **2013**, *109*, 175–196. [[CrossRef](#)]
39. Zonneveld, K.A.F.; Versteegh, G.J.M.; Kasten, S.; Eglinton, T.I.; Emeis, K.C.; Huguet, C.; Koch, B.P.; De Lange, G.J.; De Leeuw, J.W.; Middelburg, J.J.; et al. Selective Preservation of Organic Matter in Marine Environments; Processes and Impact on the Sedimentary Record. *Biogeosciences* **2010**, *7*, 483–511. [[CrossRef](#)]
40. Benner, R.; Benitez-Nelson, B.; Kaiser, K.; Amon, R.M.W. Export of Young Terrigenous Dissolved Organic Carbon from Rivers to the Arctic Ocean. *Geophys. Res. Lett.* **2004**, *31*, L05305. [[CrossRef](#)]

41. Rumolo, P.; Barra, M.; Gherardi, S.; Marsella, E.; Sprovieri, M. Stable Isotopes and C/N Ratios in Marine Sediments as a Tool for Discriminating Anthropogenic Impact. *J. Environ. Monit.* **2011**, *13*, 3399–3408. [[CrossRef](#)] [[PubMed](#)]
42. Johnston, E.L.; Mayer-Pinto, M.; Crowe, T.P. REVIEW: Chemical Contaminant Effects on Marine Ecosystem Functioning. *J. Appl. Ecol.* **2015**, *52*, 140–149. [[CrossRef](#)]
43. Pearson, A.; Hurley, S.J.; Walter, S.R.S.; Kusch, S.; Lichtin, S.; Zhang, Y.G. Stable Carbon Isotope Ratios of Intact GDGTs Indicate Heterogeneous Sources to Marine Sediments. *Geochim. Cosmochim. Acta* **2016**, *181*, 18–35. [[CrossRef](#)]
44. Darnaude, A.M.; Salen-Picard, C.; Polunin, N.V.C.; Harmelin-Vivien, M.L. Trophodynamic Linkage between River Runoff and Coastal Fishery Yield Elucidated by Stable Isotope Data in the Gulf of Lions (NW Mediterranean). *Oecologia* **2004**, *138*, 325–332. [[CrossRef](#)]
45. Meyers, P.A. Preservation of Elemental and Isotopic Source Identification of Sedimentary Organic Matter. *Chem. Geol.* **1994**, *114*, 289–302. [[CrossRef](#)]
46. Sanchez-Cabeza, J.-A.; Druffel, E.R. Environmental Records of Anthropogenic Impacts on Coastal Ecosystems: An Introduction. *Mar. Pollut. Bull.* **2009**, *59*, 87–90. [[CrossRef](#)]
47. Whitney, E.J.; Beaudreau, A.H.; Howe, E.R. Using Stable Isotopes to Assess the Contribution of Terrestrial and Riverine Organic Matter to Diets of Nearshore Marine Consumers in a Glacially Influenced Estuary. *Estuaries Coasts* **2018**, *41*, 193–205. [[CrossRef](#)]
48. Wang, X.; Li, N.; Feng, D.; Hu, Y.; Bayon, G.; Liang, Q.; Tong, H.; Gong, S.; Tao, J.; Chen, D. Using Chemical Compositions of Sediments to Constrain Methane Seepage Dynamics: A Case Study from Haima Cold Seeps of the South China Sea. *J. Asian Earth Sci.* **2018**, *168*, 137–144. [[CrossRef](#)]
49. Yang, S.; Wang, J.T. Composition and Form Distribution of Lipids Biomarkers in Surficial Sediments in Southern Coastal Area of Shandong Peninsula. *Mar. Environ. Sci.* **2012**, *31*, 11–15.
50. Wang, J.T.; Yang, S.; Tan, L.J.; Hu, J. Composition and Form Distribution of Lipids Biomarkers in a Sediment Core from Southern Coastal Area of Zhejiang Province. *Acta Oceanol. Sin.* **2011**, *33*, 83–90.
51. Guo, W.; Jia, G.; Ye, F.; Xiao, H.; Zhang, Z. Lipid Biomarkers in Suspended Particulate Matter and Surface Sediments in the Pearl River Estuary, a Subtropical Estuary in Southern China. *Sci. Total Environ.* **2019**, *646*, 416–426. [[CrossRef](#)]
52. Cordeiro, L.G.M.S.; Wagener, A.L.R.; Carreira, R.S. Organic Matter in Sediments of a Tropical and Upwelling Influenced Region of the Brazilian Continental Margin (Campos Basin, Rio de Janeiro). *Org. Geochem.* **2018**, *120*, 86–98. [[CrossRef](#)]
53. Ding, H.; Sun, M.-Y. Biochemical Degradation of Algal Fatty Acids in Oxic and Anoxic Sediment–Seawater Interface Systems: Effects of Structural Association and Relative Roles of Aerobic and Anaerobic Bacteria. *Mar. Chem.* **2005**, *93*, 1–19. [[CrossRef](#)]
54. Budge, S.M.; Parrish, C.C.; McKenzie, C.H. Fatty Acid Composition of Phytoplankton, Settling Particulate Matter and Sediments at a Sheltered Bivalve Aquaculture Site. *Mar. Chem.* **2001**, *76*, 285–303. [[CrossRef](#)]
55. Rütters, H.; Sass, H.; Cypionka, H.; Rullkötter, J. Phospholipid Analysis as a Tool to Study Complex Microbial Communities in Marine Sediments. *J. Microbiol. Methods* **2002**, *48*, 149–160. [[CrossRef](#)]
56. Yamanaka, T.; Sakata, S. Abundance and Distribution of Fatty Acids in Hydrothermal Vent Sediments of the Western Pacific Ocean. *Org. Geochem.* **2004**, *35*, 573–582. [[CrossRef](#)]
57. Zegouagh, Y.; Derenne, S.; Largeau, C.; Saliot, A. A Geochemical Investigation of Carboxylic Acids Released via Sequential Treatments of Two Surficial Sediments from the Changjiang Delta and East China Sea. *Org. Geochem.* **2000**, *31*, 375–388. [[CrossRef](#)]
58. Menzel, D.; Van Bergen, P.F.; Schouten, S.; Sinninghe Damsté, J.S. Reconstruction of Changes in Export Productivity during Pliocene Sapropel Deposition: A Biomarker Approach. *Palaeogeogr. Palaeoclimatol. Palaeoecol.* **2003**, *190*, 273–287. [[CrossRef](#)]
59. Li, X.; Liu, W.; Xu, L. Carbon Isotopes in Surface-Sediment Carbonates of Modern Lake Qinghai (Qinghai-Tibet Plateau): Implications for Lake Evolution in Arid Areas. *Chem. Geol.* **2012**, *300–301*, 88–96. [[CrossRef](#)]
60. Wang, K.; Zou, L.; Lu, X.; Mou, X. Organic Carbon Source and Salinity Shape Sediment Bacterial Composition in Two China Marginal Seas and Their Major Tributaries. *Sci. Total Environ.* **2018**, *633*, 1510–1517. [[CrossRef](#)]
61. Bao, R.; Blattmann, T.M.; McIntyre, C.; Zhao, M.; Eglinton, T.I. Relationships between Grain Size and Organic Carbon  $^{14}\text{C}$  Heterogeneity in Continental Margin Sediments. *Earth Planet. Sci. Lett.* **2019**, *505*, 76–85. [[CrossRef](#)]
62. Liu, H.; Li, Y.X.; He, X.; Sissou, Z.; Tong, L.; Yarnes, C.; Huang, X. Compound-Specific Carbon Isotopic Fractionation during Transport of Phthalate Esters in Sandy Aquifer. *Chemosphere* **2016**, *144*, 1831–1836. [[CrossRef](#)] [[PubMed](#)]
63. Wang, J.; Hilton, R.G.; Jin, Z.; Zhang, F.; Densmore, A.L.; Gröcke, D.R.; Xu, X.; Li, G.; West, A.J. The Isotopic Composition and Fluxes of Particulate Organic Carbon Exported from the Eastern Margin of the Tibetan Plateau. *Geochim. Cosmochim. Acta* **2019**, *252*, 1–15. [[CrossRef](#)]
64. Jaffé, R.; Mead, R.; Hernandez, M.E.; Peralba, M.C.; DiGuida, O.A. Origin and Transport of Sedimentary Organic Matter in Two Subtropical Estuaries: A Comparative, Biomarker-Based Study. *Org. Geochem.* **2001**, *32*, 507–526. [[CrossRef](#)]
65. Chen, J.; Li, F.; He, X.; He, X.; Wang, J. Lipid Biomarker as Indicator for Assessing the Input of Organic Matters into Sediments and Evaluating Phytoplankton Evolution in Upper Water of the East China Sea. *Ecol. Indic.* **2019**, *101*, 380–387. [[CrossRef](#)]
66. Hu, J.; Zhang, H.; Peng, P. Fatty Acid Composition of Surface Sediments in the Subtropical Pearl River Estuary and Adjacent Shelf, Southern China. *Estuar. Coast. Shelf Sci.* **2006**, *66*, 346–356. [[CrossRef](#)]
67. Birgel, D.; Stein, R.; Hefter, J. Aliphatic Lipids in Recent Sediments of the Fram Strait/Yermak Plateau (Arctic Ocean): Composition, Sources and Transport Processes. *Mar. Chem.* **2004**, *88*, 127–160. [[CrossRef](#)]
68. Xue, B.; Yao, S. Recent Sedimentation Rates in Lakes in Lower Yangtze River Basin. *Quat. Int.* **2011**, *244*, 248–253. [[CrossRef](#)]

69. Silliman, J.E.; Schelske, C.L. Saturated Hydrocarbons in the Sediments of Lake Apopka, Florida. *Org. Geochem.* **2003**, *34*, 253–260. [[CrossRef](#)]
70. Pancost, R.D.; Sinninghe Damsté, J.S.; De Lint, S.; Van Der Maarel, M.J.E.C.; Gottschal, J.C. Biomarker Evidence for Widespread Anaerobic Methane Oxidation in Mediterranean Sediments by a Consortium of Methanogenic Archaea and Bacteria. *Appl. Environ. Microbiol.* **2000**, *66*, 1126–1132. [[CrossRef](#)] [[PubMed](#)]
71. Fu, L.; Li, D.; Mi, T.; Zhao, J.; Liu, C.; Sun, C.; Zhen, Y. Characteristics of the Archaeal and Bacterial Communities in Core Sediments from Southern Yap Trench via in Situ Sampling by the Manned Submersible Jiaolong. *Sci. Total Environ.* **2020**, *703*, 134884. [[CrossRef](#)] [[PubMed](#)]
72. Thiel, V.; Peckmann, J.; Seifert, R.; Wehrung, P.; Reitner, J.; Michaelis, W. Highly Isotopically Depleted Isoprenoids: Molecular Markers for Ancient Methane Venting. *Geochim. Cosmochim. Acta* **1999**, *63*, 3959–3966. [[CrossRef](#)]
73. Hoehler, T.M.; Alperin, M.J.; Albert, D.B.; Martens, C.S. Field and Laboratory Studies of Methane Oxidation in an Anoxic Marine Sediment: Evidence for a Methanogen-Sulfate Reducer Consortium. *Glob. Biogeochem. Cycles* **1994**, *8*, 451–463. [[CrossRef](#)]